Transverse hydrodynamics of collective pion flow

Dimitri Kusnezov and George Bertsch
Department of Physics and National Superconducting Cyclotron Laboratory, Michigan State University, East Lansing, Michigan 48824
(Received 8 June 1989)

We investigate the low p_T features of the transverse momentum distribution for pions in relativistic heavy-ion collisions from the NA35 collaboration. Contrary to recent claims, we find that collective hydrodynamic flow cannot account for the experimental low p_T shape of the pion transverse momentum distribution.

Signatures of the formation of the quark-gluon plasma are the central issue in studying relativistic heavy-ion collisions. In this connection, an effect has been found in the transverse momentum spectra of pions, which has aroused much interest. As compared to spectra from NN collisions, a peak is seen at small p_T. This is present at midrapidity in the heavy-ion collision O+Au at 200 GeV/n and is seen in pA collisions at lower rapidity. The additional peaking has been interpreted as a collective flow effect in an expanding gas.[1,2] In this work we examine the hydrodynamic model in more detail, using relativistically consistent treatments of the phase-space integration and the particle distribution functions. We also use initial conditions based on Bjorken's boost-invariant cylindrical geometry,[3] which can be considered a closer approximation to the true geometry than the spherical fireball model previously employed. For a variety of initial conditions we show that the low p_T concave shape of the transverse pion distribution is inconsistent with simple transverse hydrodynamics, and hence must be accounted for elsewhere. This result is related to a general feature of the thermal distribution functions which are independent of the hydrodynamic evolution.

Hydrodynamics is used to model the complex kinetic behavior of the expanding hadron gas. The underlying assumptions are that the central region of the relativistic heavy-ion collision evolves as an ideal relativistic fluid until hadronization. When the temperature in a particular local frame of the fluid cools to a predefined freeze-out temperature T_f, hadrons have been formed and are acquiring final statistical distributions corresponding to the freeze-out temperature. The freeze-out temperature defines a three-dimensional freeze-out surface in the lab frame, outside of which the average number of collisions per hadron is less than unity. In this way a thermal distribution is folded into the hydrodynamic solutions providing a transverse particle spectra.

In this discussion we will only consider the formation of pions, with the phase-space distribution

$$dN = d^3p\, d^3x \frac{1}{e^{p^\mu u_\mu / T_f} - 1}\ , \tag{1}$$

which is manifestly Lorentz invariant. The fireball model calculations rely on the integration of this distribution or its Boltzmann limit over appropriate geometrical configurations using a velocity profile ansatz for the expanding fluid cells. The expanding spherical shell with constant β, developed in Ref. 4, has recently been applied to the low p_T region of the dN/dp_T^2 pion spectra from the NA35 collaboration.[2] In this model, a spherical shell is assumed to be expanding with constant β in the lab frame. It is natural to assume that freeze out occurs at a fixed time in the comoving frame of each fluid cell when T_f is reached, which provides a spatial freeze-out volume $dV = d^3x$ in the comoving frame of that cell. However, the model proposed in Ref. 2 consists of integrating this result over a spatial *lab* volume using the power of $\beta = \beta_0 (r/R_0)^n$ as a model parameter (for $1 \le n \le 2$). This "snapshot" assumption suggests that freeze out occurs everywhere simultaneously in the lab frame. Further, we will see below that $\beta \propto r^2$ corresponds to an incomplete integration over our freeze-out surface, and that the complete integration destroys the agreement with the low p_T data. A similar model was suggested in Ref. 1 to describe transverse momentum distributions for charged mesons in emulsion experiments. Their model consists of the integration of the Boltzmann limit of (1) over a cylindrical shell with the ansatz $\beta = \text{const}$ and only at midrapidity. The low p_T behavior of this result is also significantly modified when the integration over the entire freeze-out surface is considered. The inclusion of the finite mass of the pion will also modify the low p_T behavior of those results. Finally, the assumption of constant β in cylindrical coordinates does not lead to a closed freeze-out surface. This is clear since $\beta(r=0)=0$ by symmetry so that finite β never reaches $r=0$ for any time τ. Hydrodynamically this corresponds to a freeze-out surface with coordinates r and τ that increase with time (for sufficiently large τ), indicating that some parts of the gas will never achieve freeze out.

The geometry of the hydrodynamics of the expanding phase of a relativistic heavy-ion collision is conveniently described using Bjorken's boost-invariant cylindrical configuration,[3] which is identical to the Landau solution at midrapidity, known already for some 35 years.[5] If hydrodynamics provides the proper description of the time evolution of the central region, then this cylindrical geometry must be valid at midrapidity where the time

 ©1989 The American Physical Society

scale for longitudinal expansion is much smaller than that for transverse expansion. We begin with the usual hydrodynamic equations for the central region of the collision

$$0=D_\mu T^{\mu\nu} = \frac{\partial p}{\partial x^\mu}g^{\mu\nu}+\frac{1}{\sqrt{g}}\frac{\partial}{\partial x^\mu}[\sqrt{g}\,(p+\epsilon)u^\mu u^\nu] + \Gamma^\nu_{\mu\lambda}(p+\epsilon)u^\mu u^\lambda , \quad (2)$$

where the observer with four-velocity u_μ measures the stress-energy components

$$T^{\mu\nu}=g^{\mu\nu}p+(\epsilon+p)u^\mu u^\nu ,$$

and ϵ and p are the energy density and pressure measured in the local rest frame of the fluid. The boost-invariant cylinder in coordinates (t,r,θ,z) is characterized by the four-velocity

$$u^\mu=\gamma(t/\tau,\beta,0,z/\tau)$$

where

$$\gamma=1/(1-\beta^2)^{1/2} ,$$

$$\beta=\beta(r,\tau) ,$$

and

$$\tau=(t^2-z^2)^{1/2} .$$

Since $u_\theta=0$, the term involving the Christoffel symbol vanishes. For cylindrical coordinates $\sqrt{g}=r$ and the equations of motion can be written as

$$0=\frac{\partial E}{\partial\tau}+\frac{1}{r}\frac{\partial(rJ)}{\partial r}+\frac{E+p}{\tau}$$
$$0=\frac{\partial J}{\partial\tau}+\frac{1}{r}\frac{\partial(\beta rJ)}{\partial r}+\frac{\partial p}{\partial r}+\frac{J}{\tau} \quad (3)$$

where the lab frame energy density and radial momentum density are

$$E=\gamma^2(p+\epsilon)-p$$
$$J=\gamma^2\beta(p+\epsilon) . \quad (4)$$

We assume the equation of state for an ideal relativistic fluid $\epsilon=3p$. These equations are then solved numerically in terms of smoother evolving functions defined by $\chi=J/E$ and $\alpha=-\log E$. In this parametrization χ is a smooth function bounded on the unit interval, $0\le\chi\le1$, where $\chi=4\beta/(3+\beta^2)$. For the specific choice of $\epsilon=3p$ we have the simple relations

$$\beta=\frac{3\chi}{2[1+(1-\frac{3}{4}\chi^2)^{1/2}]} ,$$
$$p=E\frac{2(1-\frac{3}{4}\chi^2)^{1/2}-1}{3} . \quad (5)$$

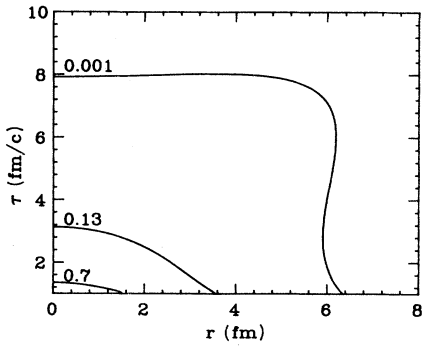

FIG. 1. Freeze-out surfaces in the $r-\tau$ plane using Gaussian initial conditions and $\tau_i=1$ fm/c for local frame final energy densities $\epsilon_f/\epsilon_i=0.7$, 0.13, and 0.001.

The equations (3) written in terms of χ and α are then evolved until freeze out, which is defined by a temperature T_f. We assume freeze out occurs in each local frame when $\epsilon_f=(T_f/T_i)^4\epsilon_i$, although the qualitative features of the pion distribution do not depend strongly on the profile of the freeze-out surface in the $r-\tau$ plane.

Since the precise nature of the initial conditions is not completely understood, we have considered a variety of initial conditions. The initial time at which the hydrodynamic phase begins to evolve was studied from 0.1 fm $\le\tau_i\le$ 5 fm and the freeze-out temperature T_f from 100–300 MeV. The initial energy density distribution at τ_i was then varied from a smoother Gaussian distribution to a more abruptly changing Fermi-Dirac distribution (a finite surface thickness is needed to avoid numerical oscillations). We have also taken freeze-out surfaces where the local energy density is in the range $0.001\le\epsilon_f/\epsilon_i\le1.0$. For all these conditions we take the initial momentum density $J(r,t=0)=0$ and $\beta(r,t=0)=0$. In this wide range of initial conditions the transverse pion distributions we find are qualitatively identical. Further, the qualitative features of the pion distribution do not depend strongly on the profile of the freeze-out surface in the $r-\tau$ plane. A typical family of freeze-out contours for the Gaussian energy density initial condition is illustrated in Fig. 1. Analogous contours for Fermi-Dirac distributions can be found in Ref. 10.

The statistical distribution of the pions is folded into the freeze-out surface σ using a more general statement of Eq. (1). The distribution of particles in a general three volume can be written in the Lorentz-invariant form[6,7]

$$p_0\frac{dN}{d^3p}=\frac{1}{e^{p^\mu u_\mu}-1}p^\mu d\sigma_\mu . \quad (6)$$

For a spatial freeze-out volume $d\sigma_0=d^3x$ in the local frame this reproduces Eq. (1). The transverse distribution can then be obtained by numerical integration of (6). In terms of the longitudinal rapidity η and particle rapidity y, the resulting integral is of the form[7,10]

$$\frac{dN}{dp_T^2}=\frac{g}{8\pi^2}\int_y dy\int_{-\infty}^{\infty}d\eta\int_0^{2\pi}d\theta\int_s ds\,\tau r\frac{\left[m_T\cosh(\eta-y)\frac{dr}{ds}-p_T\cos\theta\frac{d\tau}{ds}\right]}{\exp[(\gamma m_T\cosh(\eta-y)-p_T\gamma\beta\cos\theta)/T_f]-1} . \quad (7)$$

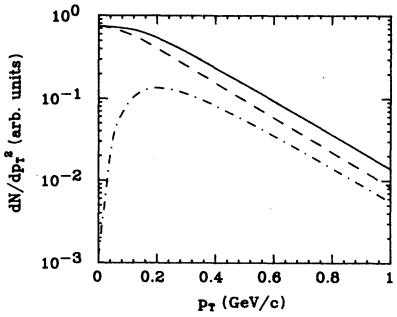

FIG. 2. Breakdown of the thermal distribution integrals [cf. Eq. (7)] for transverse pions into the dr (dashed) and $d\tau$ (dot-dashed) components. The dr contribution corresponds to the results obtained in Ref. 2, whereas the complete integral has zero slope at $p_T=0$. The total integral, shown by the solid curve, does not exhibit the strong peak seen in the experimental data at low momentum. These results are based on $\epsilon_f/\epsilon_i=0.13$ and $T_f=100$ MeV, although the results are qualitatively identical for all the freeze-out surfaces of Fig. 1, as well as for Fermi function initial conditions.

Here s is the arclength on the $\tau-r$ component of the freeze-out surface,

$$m_T=(m_\pi^2+p_T^2)^{1/2} ,$$

and γ, β, τ, and r are functions of s. The two components of a typical integration of Eq. (7) are illustrated in Fig. 2. For massive particles, the $d\tau$ integral vanishes at $p_T=0$. The dr integral alone corresponds to the results obtained in Ref. 2. This is displayed in Fig. 3, where the models of Ref. 1 (dot-dashed curve) and Ref. 2 (dashed curve) and Eq. (7) (solid) are compared to the O+Au data from the NA35 collaboration.[8] The slope of Eq. (7) agrees with the data at a temperature of $T_f=80$ MeV, the same temperature found in Ref. 9 using the Landau-Milekhin model. The corresponding dr contribution to this integral has been renormalized in order to lie on the experimental curve, and overlaps with the results of Ref. 2 (dashed curve). Hence the dashed curve corresponds to both the dr integral and the results of Ref. 2. The low p_T excess is clearly evident. At larger p_T, as has been detailed in previous hydrodynamic studies, the thermal distribution (7) is generally concave up above 0.5 GeV/c, analogous to Refs. 1 and 2.[10]

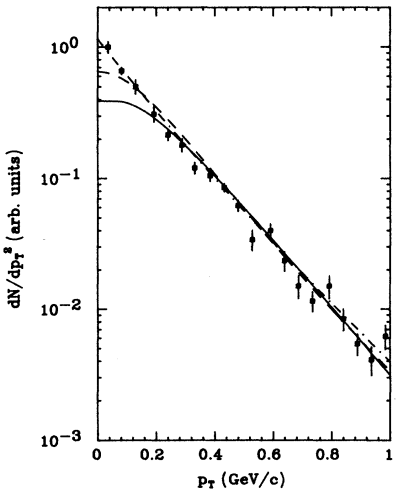

FIG. 3. Comparison of the distributions obtained in Ref. 1 (dot-dashes), Ref. 2 (dashes), and Eq. (7) (solid) to the NA35 data (Ref. 8). The dr integration contribution to Eq. (7) coincides with the results of Ref. 2 (dashes). The dot-dashed curve corresponds to the parameters $\beta=0.4$ and $T_f=150$ MeV, and the solid curve corresponds to $T_f=80$ MeV, $\tau_i=1$ fm, and $\epsilon_f/\epsilon_i=0.13$.

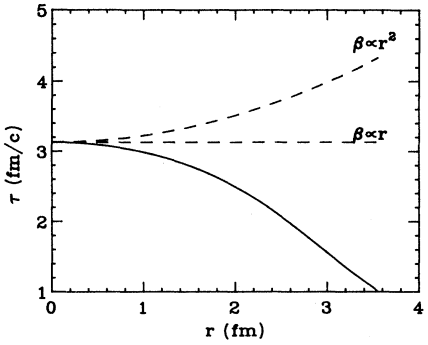

FIG. 4. Freeze-out surfaces obtained with the boost-invariant cylindrical geometry (solid) compared to the surface implicitly assumed in the formulation in Ref. 2 (dashed). The dashed freeze-out surface corresponds to a "snapshot" freeze out in the lab frame which selects the dr integration in Fig. 2.

It is interesting to examine the nature of the freeze-out ansatz $\beta\propto r^n$ in this framework, since this is employed in Ref. 2. For the case of Gaussian initial conditions, $\beta(r,\tau)$ is roughly linear with r for τ not too large. (In the case of a Fermi function initial condition β is roughly quadratic in r.) The freeze-out surfaces corresponding to $\beta\propto r^n$ for $n=1,2$ are indicated in Fig. 4. It is clear that in choosing the ansatz and integrating over a spatial lab freeze-out volume, the result is equivalent to only the spatial integration of Eq. (7). Indeed, the neglect of $d\tau$ integral reproduces the low p_T results in Ref. 2. However, when the entire freeze-out surface is considered, the agreement

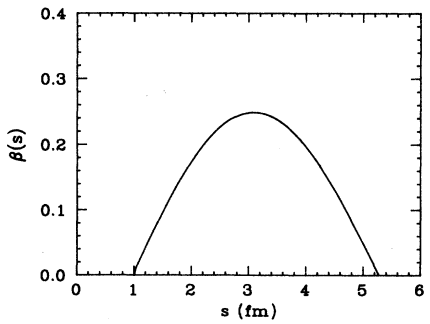

FIG. 5. The $\beta(s)$ profile at freeze out obtained for the initial conditions $\beta(r)=0$ at $\tau=0$. s in the arclength in the $r-\tau$ component of the freeze-out surface.

is much poorer in the low p_T region, as indicated in Figs. 2 and 3. Let us consider the $\beta(s)$ profile obtained in Bjorken's geometry, where s is the freeze-out surface proper time. Since the initial energy density distribution will have a tail in the radial direction, there is already freeze-out at finite r at $\tau=0$, for which $\beta=0$. By symmetry, $\beta=0$ at the origin, so that freeze-out occurs at $r=0$ for $\beta=0$. Hence the profile of $\beta(r,\tau)$ along the freeze-out surface will be concave down, as illustrated in Fig. 5. [For Gaussian initial conditions $\beta(r)$ resembles an inverted parabola.] This argument depends on our initial condition that $\beta(r)=0$ for $\tau=0$. Since the hydrodynamic phase can begin at times of order 1 fm/c, deviations from this initial condition might be expected for $r\sim r_N$, where r_N is the radius of the lighter nucleus. Nevertheless, the $\beta(s)$ profile will maintain the concave down form (similar to an inverted parabola), the only difference being that for $\tau=0$, β has a nonzero value. It is noteworthy that the distribution function Eq. (7) maintains a zero slope at $p_T=0$, independent of the freeze-out contour, provided the particles have a finite mass. If we take $m_\pi=0$, then there is nonzero slope at the origin, and we obtain the results of Ref. 10.

In conclusion, we have shown that previous studies which find agreement with the concave shape of the low p_T component of the dN/dp_T^2 spectra correspond to incomplete descriptions of the hydrodynamic evolution and that a more complete description provides poorer agreement with the data. Further, the velocity ansatz that have been used result in unnatural assumptions concerning the nature of the freeze-out surface. Our conclusion is also supported by recent studies in the Cascade model.[11] Since collective hydrodynamic expansion is not sufficient to describe these effects, one can only speculate that the structure may be due to internal degrees of freedom that are not modeled in this way, such as supercooled glueballs or the possibility of a quark-gluon plasma. Another possible explanation, that the pions originate from the decay of baryon resonances, seems insufficient to explain the observations at midrapidity.[12]

We acknowledge useful discussions with Aurel Bulgac and Pawel Danielewicz. Support for this work was provided by the National Science Foundation under Grant No. 87-14432.

[1]T. W. Atwater, P. S. Freier, and J. I. Kapusta, Phys. Lett. B **199**, 30 (1987).
[2]K. S. Lee, M. J. Rhoades-Brown, and U. Heinz, Phys. Rev. C **37**, 1463 (1988); K. S. Lee and U. Heinz, Z. Phys. C **43**, 425 (1989).
[3]J. D. Bjorken, Phys. Rev. D **27**, 140 (1982).
[4]P. J. Siemens and J. O. Rasmussen, Phys. Rev. Lett. **42**, 880 (1979).
[5]L. D. Landau, in *Collected Papers of Landau,* edited by D. ter Haar (Gordon-Breach, London, 1965), p. 569.
[6]W. Israel, J. Math. Phys. **4**, 1163 (1963).
[7]F. Cooper, G. Frye, and E. Schonberg, Phys. Rev. D **11**, 192 (1975).
[8]J. W. Harris *et al.*, Nucl. Phys. **A498**, 133c (1989); H. Ströbele *et al.*, Z. Phys. C **38**, 89 (1988).
[9]R. Venugopalan and M. Prakash, State University of New York Report NTG-89-17, 1989.
[10]M. Kataja, P. V. Ruuskanen, L. D. McLerran, and H. von Gersdorff, Phys. Rev. D **34**, 2755 (1986); P. V. Ruuskanen, Acta. Phys. Pol. B **18**, 551 (1986).
[11]G. Bertsch, M. Gong, L. McLerran, V. Ruuskanen, and E. Sarkkinen, Phys. Rev. D **37**, 1202 (1988).
[12]G. Bertsch and G. E. Brown, Phys. Rev. C **40**, 1830 (1989).